JAC Antimicrob Resist
https://doi.org/10.1093/jacamr/dlaf045

JAC-Antimicrobial Resistance

Enhancing biofilm disruption and bactericidal efficiency using vancomycin-loaded microbubbles in sonodynamic therapy

Wen B. Mu[1,2], Li Q. Yao[3], Zi Y. Guo[2], You C. Ma[3], Fei Wang[2] and Jian H. Yang[1,4]*

[1]Department of Pharmacognosy, School of Pharmacy, Xinjiang Medical University, Urumqi, Xinjiang 830011, China; [2]Department of Orthopaedics, First Affiliated Hospital of Xinjiang Medical University, Urumqi, Xinjiang 830054, China; [3]Department of Sports Medicine, First Affiliated Hospital of Xinjiang Medical University, Urumqi, Xinjiang 830054, China; [4]Department of Pharmacy, State Key Laboratory of Pathogenesis, Prevention and Treatment of High Incidence Diseases in Central Asia, The First Affiliated Hospital of Xinjiang Medical University, Urumqi, Xinjiang 830011, China

*Corresponding author. E-mail: yjh_yfy@163.com

Received 21 November 2024; accepted 6 March 2025

Background: Periprosthetic joint infection (PJI) is a significant complication following arthroplasty, attributed to the biofilm formation. This study evaluates the effectiveness of vancomycin-loaded microbubbles (Van-MBs) in conjunction with ultrasound-targeted microbubble destruction (UTMD) on biofilm disruption and bactericidal efficiency.

Methods: Van-MBs were prepared using the thin-film hydration method and characterized using microscopy, dynamic light scattering analysis, and high-performance liquid chromatography (HPLC). Confocal laser scanning microscopy (CLSM) was used to assess the penetration of Van and Van-MBs into biofilms. Biofilms were treated with Van, Van-MBs, UTMD, and Van-MBs + UTMD. CLSM and crystal violet staining were utilized to assess the morphology, viability, and biomass of the biofilms. Bacterial activity was examined through scanning electron microscopy (SEM) and plate counting, while gene expression was analyzed using quantitative real-time polymerase chain reaction (qRT-PCR).

Results: The results demonstrated that Van-MBs penetrated deeper into methicillin-resistant *Staphylococcus aureus* (MRSA) biofilms compared with Van alone. The combination of Van-MBs and UTMD significantly reduced biofilm thickness, viability, and biomass. qRT–PCR analysis revealed that the Van-MBs + UTMD group exhibited lower transcription levels of the icaA gene, suggesting that the treatment disrupted biofilm formation by suppressing this key gene. SEM further confirmed the efficacy of the treatment, showing that Van-MBs + UTMD induced cytoplasmic shrinkage and separation of the outer and cytoplasmic membranes in MRSA cells, indicating substantial structural damage to the bacterial cells.

Conclusion: These findings demonstrate the potential of Van-MBs in combination with UTMD as an innovative approach to enhance antibiotic efficacy and eliminate biofilms in the treatment of PJI.

Introduction

Periprosthetic joint infection (PJI) is a serious complication following joint surgery, and its incidence is rising with the increasing number of surgical procedures performed. Biofilms have been identified as a primary factor in the development of PJI.[1,2] Biofilms are aggregates of microbial cells that adhere to surfaces, such as prostheses or internal fixation devices, due to the presence of extracellular polymeric substances (EPS).[3] These biofilms are responsible for approximately 80% of chronic and recurrent infections, presenting significant treatment challenges.[4,5]

Antibiotics are often ineffective against biofilm-associated infections due to their inability to penetrate the dense biofilm matrix and their susceptibility to deactivation by biofilm surface substances.[6] As a result, PJI patients frequently require prolonged, high-dose antibiotic regimens, which increase the risk of toxicity. When antibiotic therapy fails, severe complications can arise, often necessitating surgical intervention, although

complete biofilm removal is not guaranteed.[7] Therefore, there is an urgent need for innovative therapies to enhance antibiotic efficacy or eliminate biofilms.

Ultrasound-targeted microbubble destruction (UTMD) has emerged as a promising approach. UTMD combines contrast agent microbubbles with ultrasound to deliver exogenous substances to a targeted area efficiently and non-invasively. This method can disrupt dense connective tissue and cell membranes, enhancing therapeutic effects and offering new possibilities for biofilm elimination. Additionally, research by Shayegh *et al.*[8] has shown that all methicillin-resistant *Staphylococcus aureus* (MRSA) strains contain the icaABCD gene, which is crucial for biofilm formation.

Based on the above, the current study investigated the use of ultrasound-targeted vancomycin-loaded microbubbles (Van-MBs) to disrupt MRSA biofilms associated with the icaABCD gene (Figure 1). The research aims to investigate the antimicrobial efficacy of this method and explore the mechanisms underlying its ability to disrupt biofilms, thereby providing a deeper understanding of its therapeutic potential.

Materials and methods

Preparation of the Van-MBs

Van-MBs were made using the thin-film hydration method.[9] 1,2-distearoyl-sn-glycero-3-phosphocholine and 1,2-distearoylsn-glycero-3-phosphoethanolamine-N-[methoxy (polyethylene glycol)-2000] (DSPE-PEG2000) (Corden Pharma, Inc, Liestal, Switzerland) were dissolved in chloroform at a 9:1 molar ratio. One milligram of Van (Sigma–Aldrich) was dissolved in normal saline. The three solutions were fully dissolved and mixed, and the mixed solution was evaporated with a stable nitrogen flow and then dried under vacuum. The obtained lipid film was resuspended in 0.1 M TBS (pH 7.4) at a ratio of 10:10:80 (v/v/v) at 65°C. The lipid solution was divided into vials (1 mL each). After sealing, the vials were vacuumed and filled with perfluoropropane (C_3F_8) gas. The solution was mixed with a silver-mercury capsule for 30 s to obtain a Van-MBs suspension. MBs were also made without van. Van (Sulfo-Cyanine5)-MBs (DiI) were prepared similarly using 1,1′-dioctadecyl-33,3′, 3′-tetramethylindocarbocyanine perchlorate (Beyotime, Haimen, China). The basic composition of these MBs consists of a C_3F_8 gas core, surrounded by a membrane layer formed by lipids.

Characterization of the Van-MBs

The shapes of the MBs and Van-MBs were analyzed using a microscope. Van (Sulfo-Cyanine5)-MBs (DiI-labeled MBs) were viewed via confocal laser scanning microscopy (CLSM) (Leica, Germany). A dynamic light scattering analysis (Zetasizer Nano ZS, UK) was utilized to measure the size, potential, and dispersion index of the MBs and Van-MBs. The Van content within the MBs was quantified using high-performance liquid chromatography (HPLC, Agilent, USA) through an indirect quantification method. The procedure involved the following steps: (i) a known total amount of Van was added to the MBs; (ii) the residual Van concentration in the external solution was measured; and (iii) the encapsulated Van was calculated by subtracting the detected external Van concentration from the initial total amount of Van added. This methodology ensured an accurate assessment of the Van content within the MBs. The mobile phase used was an Agilent TC-C18 column (250.0 mm × 4.6 mm, 5 μm). It consisted of acetonitrile and a 0.0125 mol/L phosphoric acid solution (pH 3.2, 10:90 ratio) at a flow rate of 1 mL/min. The column temperature was 35°C, and the detection wavelength was 236 nm. A 10 μL sample was used for analysis.[10] Drug encapsulation and drug loading efficiencies were calculated using the following formulas:

Drug encapsulation efficiency (%) = weight of Van in MBs/weight of the total amount of Van in preparation of MBs × 100%

Drug loading efficiency (%) = weight of Van in MBs/weight of total Van-MBs × 100%

UTMD-triggered Van release

An ultrasound probe (Sonitron 2000V, Japan) triggered the release of Van from the Van-MBs. Five hundred microliters of Van-MBs (10^6 pieces/mL) were injected into a 5 mm agarose mold chamber. The Van-MBs were destroyed by UTMD (frequency = 1.7–3.4 MHz; duty cycle = 50%; mechanical index = 0.6) with a 2 min irradiation time.[11] The optimized UTMD parameters were used in all the following experiments. The sonicated samples were then collected and centrifuged for 5 min at 1000 rpm. The supernatant was analyzed by HPLC to measure the Van released from the Van-MBs.

Bacterial strains and biofilm formation

MRSA (USA300, ATCC, USA) was grown overnight at 37°C with shaking (180 rpm/min) in 6 mL of TSB supplemented with 0.5% dextrose. The bacteria were harvested and resuspended in TSB + 0.5% dextrose at a turbidity of 0.5 McFarland. MRSA biofilms were developed in 6-well plates, confocal dishes, and cell-climbing tablets (Thermo Fisher LabServ, Massachusetts, USA). Bacteria suspension (2 mL) at 0.5 McFarland was added into 6-well plates, confocal dishes, and cell-climbing tablets incubated at 37°C for 24 h. Bacteria adhered to the bottom and formed biofilms.

Minimum inhibitory concentration, MBC and minimum biofilm eradication concentration

The antimicrobial effect of Van was tested by diluting it in Mueller-Hinton broth. Dilutions ranging from 32 to 0.5 mg/L were prepared. The minimum inhibitory concentration (MIC) and minimum bactericidal concentration (MBC) for Van were determined using the methods of Kot *et al.*[12] Each well with a biofilm received Van at various concentrations (200 μL) and was then incubated for 24 h at 37°C. The medium was removed, and the biofilms were washed twice with 250 μL of sterile PBS. Crystal violet stain was then added to each well, and the microplates were incubated for 8 min at room temperature.[13] The lowest Van concentration with no color change was the MBEC value.

Penetration of Van and Van-MBs into MRSA biofilms

After 24 h of biofilm growth, the supernatant was replaced with either 100 μL of 32 mg/L vancomycin (Cy5-labeled Van) or 10^6 pieces/mL Van-MBs (DiI-labeled). The biofilms were then incubated for 5 min at room temperature and washed with 1 mL of double-distilled water to remove excess Van or Van-MBs. CLSM revealed Van or Van-MBs in biofilms, and their penetration was assessed. Additionally, Van or Van-MB concentrations that penetrated biofilms were compared. Bacteria were stained with SYTO9 (Thermo Fisher Scientific, USA) and excited at 480/500 nm to visualize biofilms.

Treatment of biofilms

MRSA biofilms were treated with Van (32 mg/L), MBs (10^6 pieces/mL) or Van-MBs (10^6 pieces/mL). Biofilms were randomly divided into five groups: control, Van, Van-MBs, UTMD and Van-MBs + UTMD. Biofilms were stained with SYBR Green I (Thermo Fisher Scientific, USA).[14] Biofilm morphology and structure were observed using CLSM and analyzed with Image J to assess viability. The biomass of the biofilm was obtained using the crystal violet staining method. In brief, the biofilm was stained with crystal violet and then fixed with 100% methanol. After fixation, the stained biofilm was dissolved using 30% acetic acid, and the

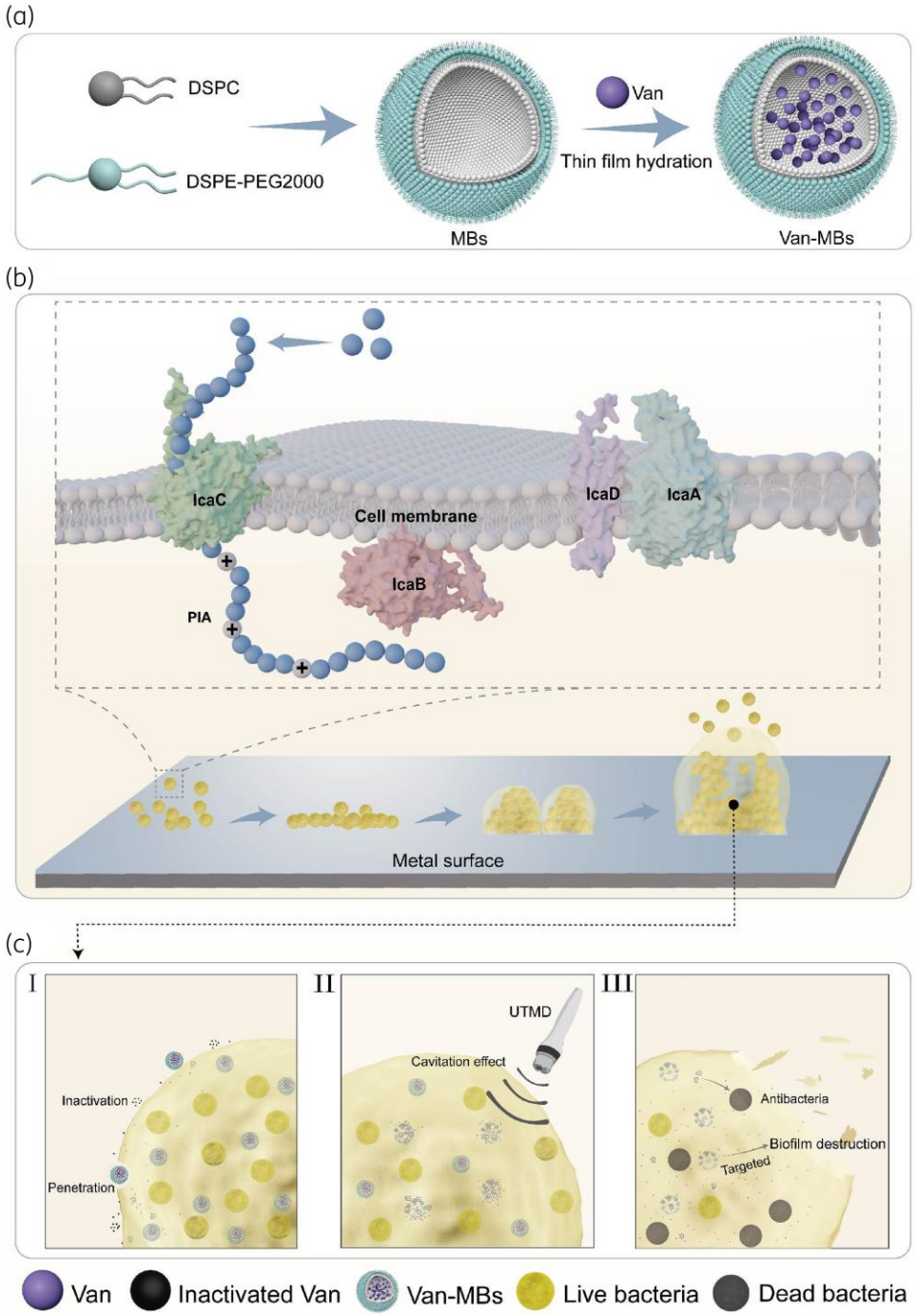

Figure 1. Schematic image illustrating Van-MBs combined with US to disrupt biofilms and kill bacteria *in vitro*. PIA, polysaccharide intercellular adhesin; UTMD, ultrasound-targeted microbubble destruction; Van, vancomycin; Van-MBs, vancomycin-microbubble.

optical density corresponding to the biofilm biomass was measured using a microplate reader. Plate counting was used to determine cfu counts for live bacteria in the biofilm. Bacterial cell morphology was visualized on cell-climbing slides. Various treatments were applied before fixing the cells with a 2.5% glutaraldehyde solution for 4 h and dehydrating them for 15 min with ethanol at different concentrations (50%, 70%, 80%, 90% and 100%). The samples were then subjected to gold sputtering to enhance conductivity. Bacterial morphology was subsequently observed using a scanning electron microscope (SEM) (Leica, Germany).

Gene expression experiment

The biofilm was subjected to diverse treatments and collected by centrifugation. Following three times washes, total bacterial RNA was isolated

with the Bacteria RNA Extraction Kit (Vazyme, Nanjing, China). mRNA was reverse transcribed to cDNA using the Color Reverse Transcription Kit (EZBioscience, Roseville, MN, USA) along with a 2× Color SYBR Green qPCR master mix (EZBioscience). The relative gene expression level was assessed utilising the $2^{-\Delta\Delta Ct}$ method with 16S rRNA as the internal reference gene.[15,16] The primer sequences for target gene amplification are detailed in Table 1.

Statistical analysis

SPSS 25 (SPSS, Chicago, IL, USA) was used to analyze the data. The Shapiro–Wilk test was used to check for normality. ANOVA and *t*-tests were used for normally distributed data, while Kruskal–Wallis and Mann–Whitney *U*-tests were used for non-normally distributed data. A P value < 0.05 was considered to indicate statistical significance.

Results

Characterization of MBs, Van-MBs and Van release under UTMD

Figure 2a shows bright-field images of MBs and Van-MBs. Microscopy images revealed that all MBs and Van-MBs were spherical and dispersed. CLSM images showed that Van was successfully encapsulated within the MBs (Figure 2b). Zeta potential analysis indicated that the average sizes of the MBs and Van-MBs were 514.0 ± 12.994 nm and 570.9 ± 9.845 nm, respectively (Figure 2c). The zeta potential increased from 0.79 ± 0.253 mV to 2.49 ± 0.755 mV in the Van-MBs group (Figure 2d). The polydispersity indices for the MBs and Van-MBs were 0.398 ± 0.023 and 0.238 ± 0.037, respectively (Figure 2e). HPLC was used to assess standard Van solution, and an absorption peak at 236 nm was detected (Figure 2f). The peak area-concentration standard curve for Van was plotted (Figure 2j). The separation of Van-MBs from the supernatant was carried out using a 0.22 μm filtration process. This process involved several steps: first, the prepared Van-MBs were thoroughly mixed using a silver-mercury amalgamator to ensure uniform dispersion. Next, the homogenized mixture was drawn into a syringe and passed through a 0.22 μm filter membrane. Finally, the resulting filtrate, which was free of MBs, contained Van in its free form. The residual Van concentration in the supernatant determined an encapsulation efficiency of $86.03 \pm 0.061\%$ and a drug loading efficiency of $25.913 \pm 0.184\%$. The controlled release of Van from Van-MBs by UTMD was achieved, with a release concentration of 34.0 ± 0.4 mg/L.

Table 1. Sequences of primers designed for qRT–PCR analyses

Genes	Sequences of primers
icaA	F:TACGTTGTCTAATGTTCTTGC
	R:AGTATCTGCATCCAAGCAC
icaB	F:TGCAGATGACGATTCACC
	R:TAGCATCATGTGATTTTAGCC
icaC	F:TCTTGTCACAGTTACTGACAACC
	R:TACCATTGACCTAATAGGAC
icaD	F:AGAGAAACAGCACTTATCGC
	R:AGCAACACGTATTGTATTG
rRNA	F:CGGCCTAACTACGTGCCAGCAGC
	R:GCGCTTTACGCCCAATAATTCC

F, forward primer; R, reverse primer.

Antibacterial activity of Van against the MRSA strain

We reviewed the antibacterial effects of Van on different *S. aureus* strains. We also assessed Van's MIC and MBC against planktonic USA300 bacteria and the MBEC against USA300 bacterial biofilms (Table 2).

Penetration of Van and Van-MBs into biofilms

Confocal laser microscopy was used to study Van and Van-MBs penetration into MRSA biofilms on collagen-coated glass slides. Van seemed to only attach to the surface of the biofilms, and bacteria in the deepest layers showed little red fluorescence (Figure 3a). In contrast, when Van-MBs were added to the biofilm, deeper layers became fluorescent (Figure 3b). Compared with Van alone, Van-MBs penetrated significantly deeper into the biofilm ($P < 0.05$) (Figure 3c).

Biofilm elimination and mechanism

3D CLSM showed that the control group biofilms were dense and that the Van and Van-MBs groups were stable. The UTMD and Van-MBs + UTMD groups had loosened structures and increased microporosity, which was most pronounced in the Van-MBs + UTMD group (Figure 4a–e). Biofilm thickness and viability were analyzed using CLSM images and Image J software. Compared with those in the control and Van groups, the biofilm thickness in the Van-MBs + UTMD group decreased (Figure 4f). Green fluorescence in CLSM images indicated lower biofilm viability after treatment with Van-MBs + UTMD than after treatment with the other groups (except for the UTMD group) (Figure 4g). Biofilm removal was confirmed with crystal violet staining. The biomass in the different groups differed significantly from that in the Van-MBs + UTMD group, indicating effective biofilm disruption through physical destruction and antibiotic treatment ($P < 0.05$).

The qRT–PCR results showed that the Van-MBs + UTMD group had lower icaA transcription than the control group ($P < 0.05$). No significant differences were detected among the other groups ($P > 0.05$). The expression levels of icaB, icaC and icaD were similar among the groups ($P > 0.05$) (Figure 5).

Antimicrobial assays and antimicrobial mechanism

CLSM revealed live green bacteria and dead red bacteria (Figure 6a). Quantitative analysis was used to determine the proportion of live bacteria in the total population. As shown in Figure 6b, the group treated with Van-MBs + UTMD exhibited greater bacterial cell death than the other groups ($P < 0.05$). This was confirmed by colony-forming unit enumeration. The Van group, which was only treated with antibiotics, had a modest 30.77% inactivation rate, showing that the use of antibiotics alone is not enough against MRSA. In contrast, the Van-MBs + UTMD treatment group had the greatest reduction in bacterial viability, which was much greater than the reductions observed in the Van-MBs (51.35%) or UTMD groups (55.38%) alone (Figure 6c).

To explain how Van-MBs + UTMD treatment works, we used SEM to observe changes in microorganisms. Figure 7 shows

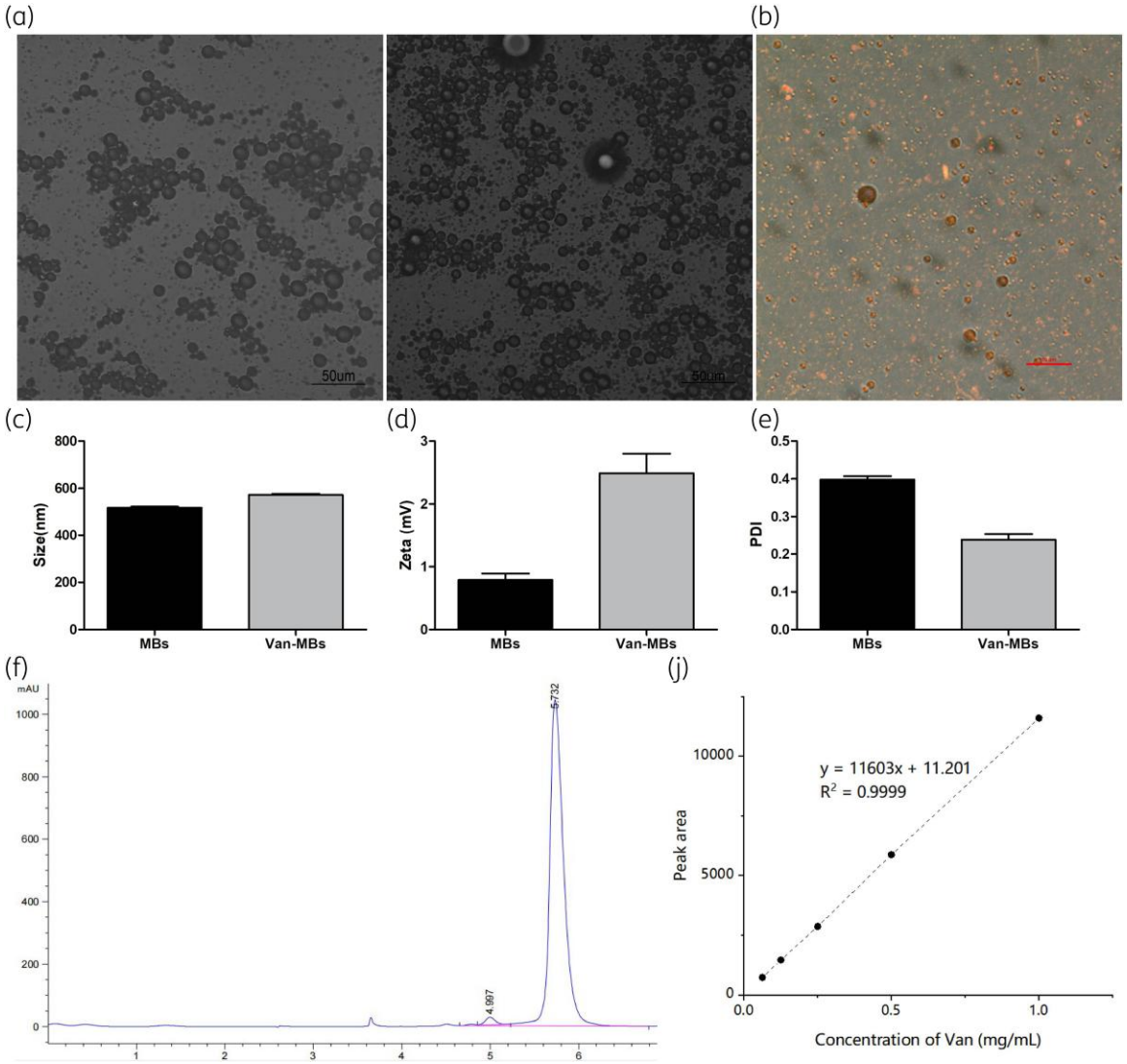

Figure 2. Characterization of Van-MBs and UTMD-triggered Van release. (a) Bright-field microscopy images of MBs and Van-MBs. (b) CLSM image of Van-MBs. (c) Particle size of MBs and Van-MBs. (d) Zeta potential of MBs and Van-MBs. (e) Dispersion indices of MBs and Van-MBs. (f) Van high-performance liquid chromatograms. (j) The peak area-concentration standard curve for Van. The values represent the means plus SDs of three measurements.

Table 2. MIC, MBC and MBEC values of Van for *S. aureus* strains

S. aureus strains	MIC (mg/L)	MBC (mg/L)	MBEC (mg/L)
ATCC49230	2	—	>8000[17]
ATCC BAA-1556	2	—	>8000
ATCC6538P	0.5	0.5	>2000[18]
MRSA16	1	1	>2000
ATCC29213	1	1–2	>1024[19]
UOC18	1–2	1–2	>1024
USA300	2	8	>8192

ATCC BAA-1556, UOC18 bacteria belong to the MRSA strain.
MBC, minimum bactericidal concentration; MBEC, minimum biofilm eradication concentration; MIC, minimum inhibitory concentration.

that the MRSA bacteria in the control group maintained their round shape with smooth cell envelopes, indicating that they were alive. No significant changes were detected in MRSA cells treated with Van, Van-MBs or UTMD alone, but cells treated with Van-MBs + UTMD showed cytoplasmic shrinkage, separating the outer and cytoplasmic membranes.

Discussion

The current investigation represents the inaugural application of high-resolution CLSM to verify the encapsulation of vancomycin within microbubbles, an innovative strategy for antibiotic delivery. These Van-encapsulated MBs exhibited a superior capacity for penetrating the deeper strata of biofilms, a critical enhancement given the suboptimal performance of conventional antibiotic

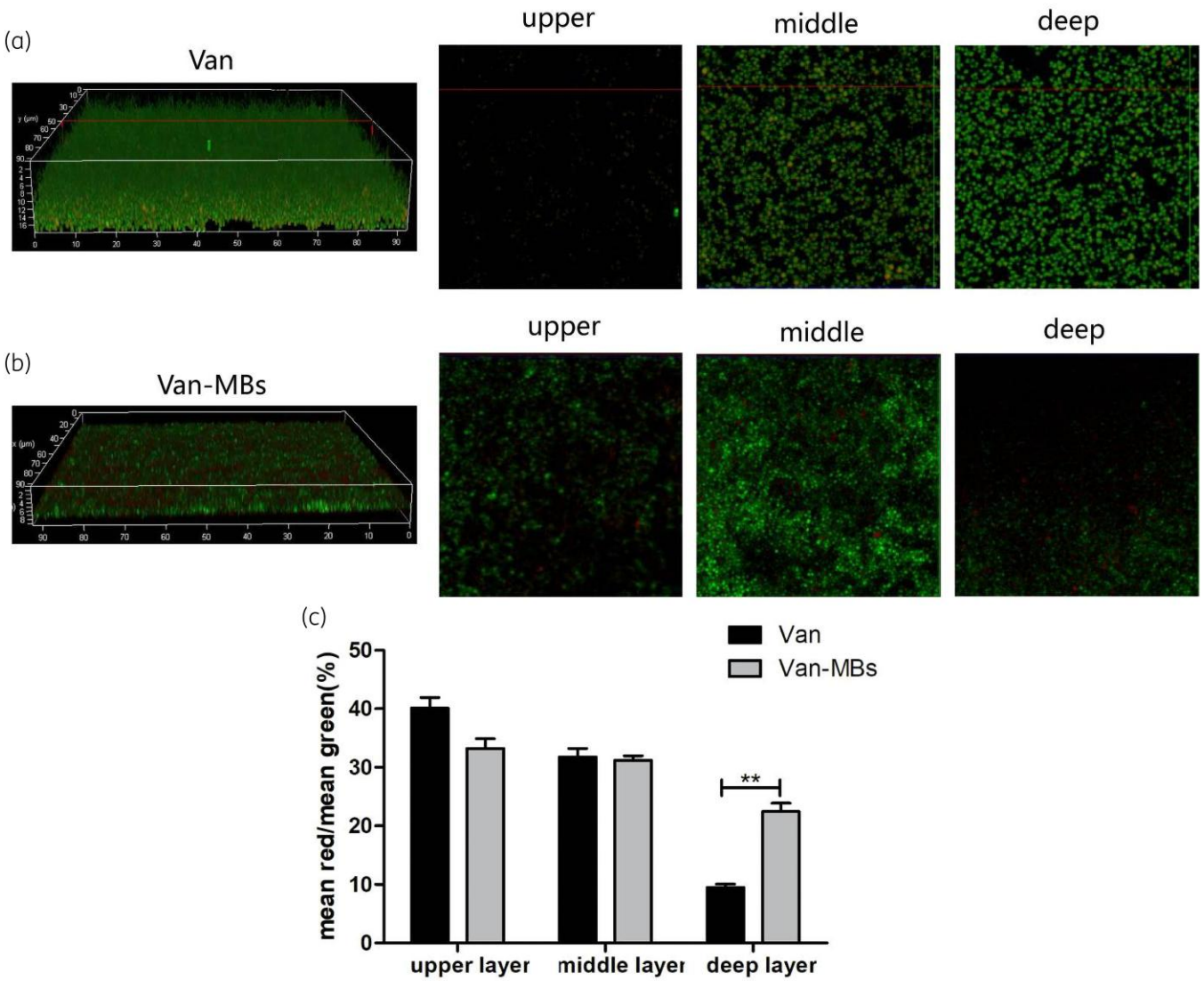

Figure 3. Confocal laser microscopy image results of the penetration of vancomycin and Van-MBs into a biofilm. (a) CLSM image results showing more Van in the upper layer and less Van in the deeper layer. (b) Observation of Van-MBs in the upper, middle and deep layers of the biofilm by CLSM. (c) Comparison of Van and Van-MBs concentrations in different layers by detecting the fluorescence intensity in the upper, middle and deep layers.

therapies against such resilient structures. The internal disruption of the biofilm, precipitated by the synergistic action of Van-MBs and ultrasound, facilitated antibiotic liberation, resulting in elevated drug concentrations at subsurface levels and thereby significantly boosting bactericidal activity. Notably, the Van concentration required to achieve effective biofilm penetration was 34.0 ± 0.4 mg/L, which is markedly lower than the established minimum biofilm eradication concentration and suggests a potential reduction in the necessary antibiotic dosage and could contribute to the attenuation of antimicrobial resistance. This approach was strategically designed to impact biofilm architecture through the suppression of icaA gene expression, which is implicated in biofilm formation. Furthermore, it elucidated a bactericidal mechanism characterized by the separation of the bacterial cell wall and plasma membrane, culminating in bacterial death.

In the present study, Van-MBs were fabricated utilising the thin-film hydration method, with subsequent high-resolution CLSM verification of successful vancomycin encapsulation. The construction of the MBs entailed a phospholipid bilayer configuration, where the hydrophilic heads were oriented internally to accommodate the hydrophilic Van, thereby circumventing the direct exposure to the biofilm that is known to precipitate antibiotic deactivation.[20] The structural integrity of the Van-MBs preserved their antimicrobial efficacy and facilitated augmented infiltration into the recalcitrant biofilm matrix. This enhanced penetration capability is likely due to the phospholipid bilayer's ability to mimic cellular membranes, which is postulated to play a role in their cellular uptake.[21] This concept aligns with the findings of Walsh *et al.*[22] who reported that liposome-encapsulated antibiotics, such as AmBisome with its amphotericin B integrated within the

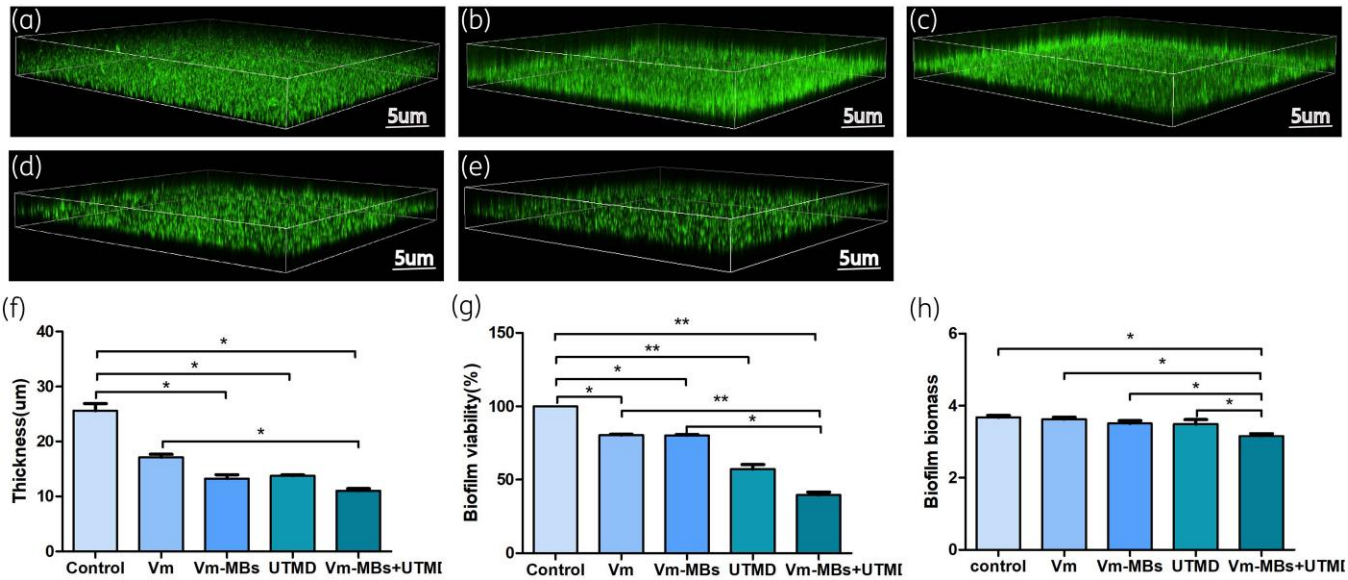

Figure 4. Effect on MRSA biofilms. Three-dimensional CLSM images of MRSA biofilms. (a) Control. (b) Van. (c) Van-MBs. (d) UTMD. (e) Van-MBs + UTMD. (f) Relative MRSA biofilm thickness after various treatments. (g) Relative MRSA biofilm viability after various treatments. (h) Crystal violet-stained MRSA biofilm biomass after various treatments. The values represent the means plus SDs of three measurements ($^{*}P < 0.05$, $^{**}P < 0.01$ compared with all other groups).

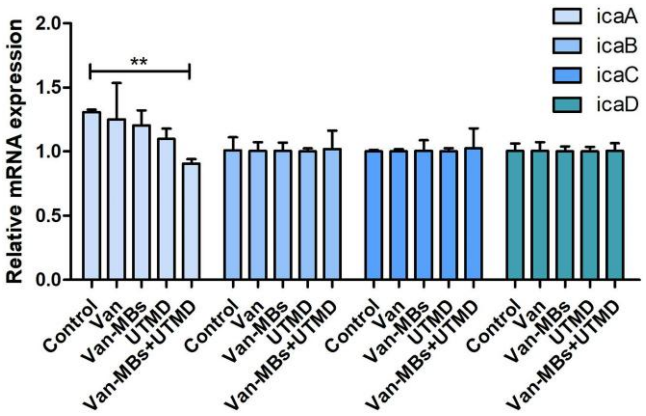

Figure 5. Transcriptional reprogramming of the icaABCD operon. Values represent the mean plus SD of three measurements ($^{*}P < 0.05$, $^{**}P < 0.01$ compared with all other groups).

lipid bilayer, exhibited superior permeability in contrast to their free counterparts in antifungal applications, underscoring the pivotal role of liposomal bilayers in mediating biofilm interactions.

The USA300 strain of MRSA, known for its clinical prevalence and resistance, demonstrated elevated MICs, MBCs and MBECs in comparison to those of other bacterial strains. The complexity of biofilms, whether they are formed on prosthetic devices or biological tissues, necessitates antibiotic dosages that are more than a 1000-fold greater than those effective against their planktonic counterparts because of the dense and intricate three-dimensional structure of biofilms, which acts as a barrier to antibiotic diffusion. Jefferson *et al.*[23] have articulated the risk associated with heightened antibiotic dosages required for biofilm penetration, which may precipitate systemic toxicity beyond the threshold of human safety. High-resolution CLSM analyses within the scope of this research revealed that the majority of non-encapsulated antibiotics were intercepted at the surface of the biofilm, failing to infiltrate and reach lethal concentrations within its internal matrix. This ineffective penetration results in antibiotics being metabolically exhausted by surface-residing bacteria over time, leading to a decrease in their effective concentration and the potential for fostering antibiotic-resistant populations within the biofilm.[23]

Our study revealed that while Van-MBs can transport Van into deeper biofilm layers, the encapsulated antibiotic requires external force to be activated and thus lacks significant bactericidal efficacy on its own. UTMD treatment alone disrupted the biofilm but had limited bactericidal impact; antibiotics are still required for sterilisation. Kouijzer *et al.*[10] successfully used a 'two-step process' combining MBs with ultrasound for biofilm disruption followed by antibiotic administration. However, limitations exist in this approach's bactericidal efficacy due to the presence of EPSs, which can chemically react with antibiotics, reducing their activity.[24] The MBs in this study protected the encapsulated antibiotics from inactivation and enhanced their bactericidal efficacy. The effective Van concentration was 34.0 ± 0.4 mg/L, which was significantly lower than the MBEC for various *S. aureus* strains, suggesting that this method can reduce antibiotic dosage, improving safety in clinical biofilm infection treatments.

The disruption of the structure of MRSA biofilms and bacterial eradication by this method remain underexplored. In this study, we investigated for the first time the mechanism of biofilm disruption and sterilisation. On the one hand, MRSA biofilms are orchestrated by a network that modulates gene expression for

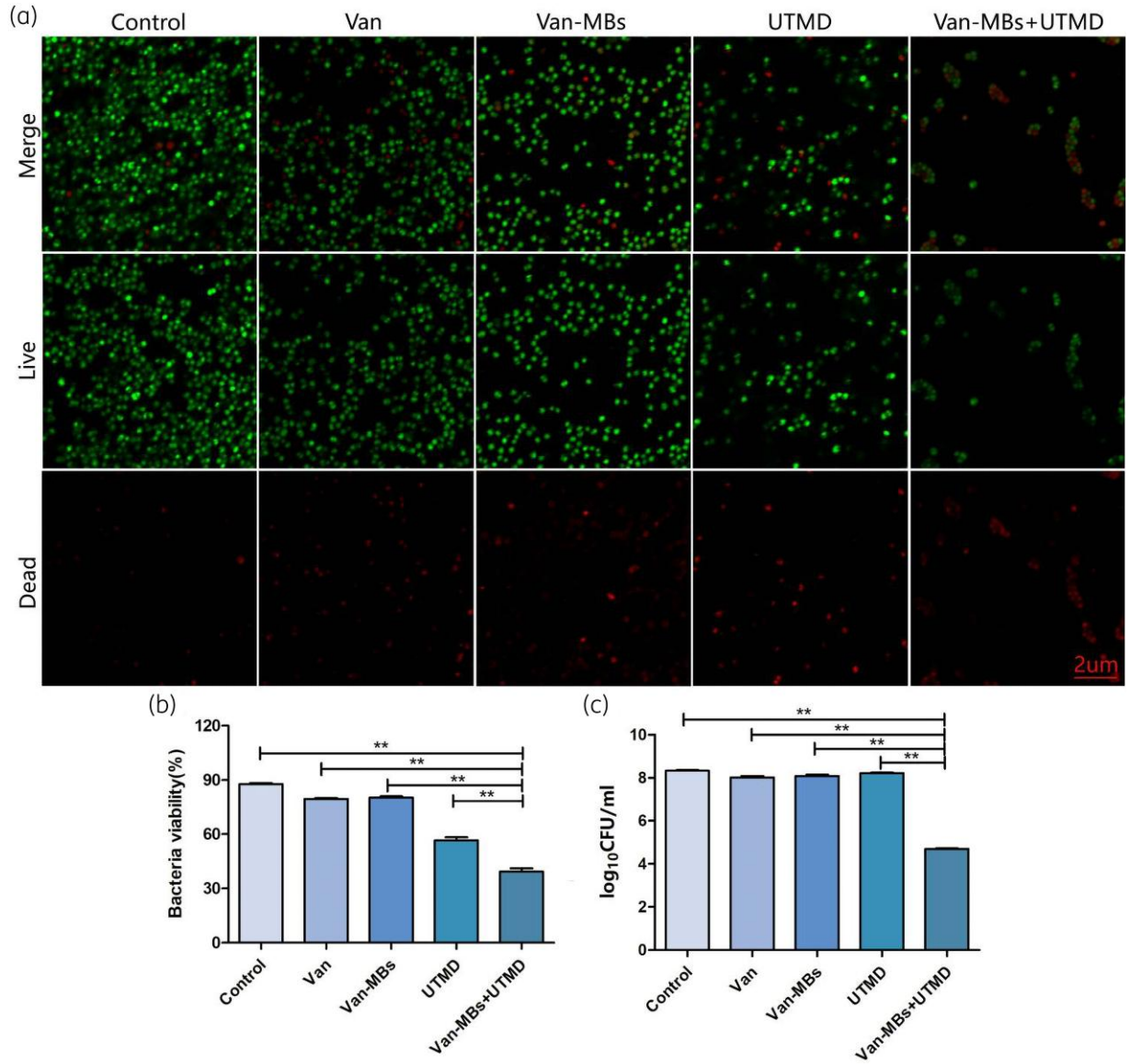

Figure 6. Antibacterial properties of Van-MBs + UTMD against MRSA bacteria. (a) Images of the live/dead bacteria assay for MRSA, in which green signals represent the surviving bacteria, while red signals indicate dead bacteria; scale bar = 2 μm. (b) Relative MRSA biofilm bacterial/viability after various treatments. (c) Relative MRSA bacterial colony counts after various treatments ($n = 3$, means ± SDs) ($^{*}P < 0.05$, $^{**}P < 0.01$ compared with all other groups).

biofilm integrity. Key regulators include the Agr system, SarA proteins, σB factor and LuxS/AI-2, which govern QS, virulence secretion, and biofilm cell dispersion.[25] The genes atlE, bap, sasG and ica also play roles in surface adherence and cell clustering.[26] This study highlights the pivotal role of the ica operon in biofilm regulation. When icaABCD genes are downregulated, PIA synthesis decreases via glucosamine aminotransferase, inhibiting biofilm formation. Conversely, upregulation of this gene enhances PIA production and biofilm development.[27] PCR results revealed reduced icaA expression, suggesting that this treatment method might impede biofilm structure by suppressing ica gene expression and PIA synthesis. The expression of other genes was unchanged, indicating that these genes play distinct roles in PIA synthesis.[28] For instance, icaA and fnbA are essential for biofilm genesis,[29] while a correlation between icaAD and mecA gene frequency exists.[8] Biofilms can also induce bacterial gene mutations, enhancing antimicrobial resistance and immune evasion.[30] On the other hand, after Van-MBs + UTMD intervention, large numbers of bacteria died, and only a few less active planktonic bacteria remained, as shown by SEM visualisation of the separation of the bacterial cell wall from the cytoplasm. This may be related to changes in the osmotic pressure of the bacterial cytoplasm.[31] Luo *et al.*[32] study suggested that ion channel dysfunction,

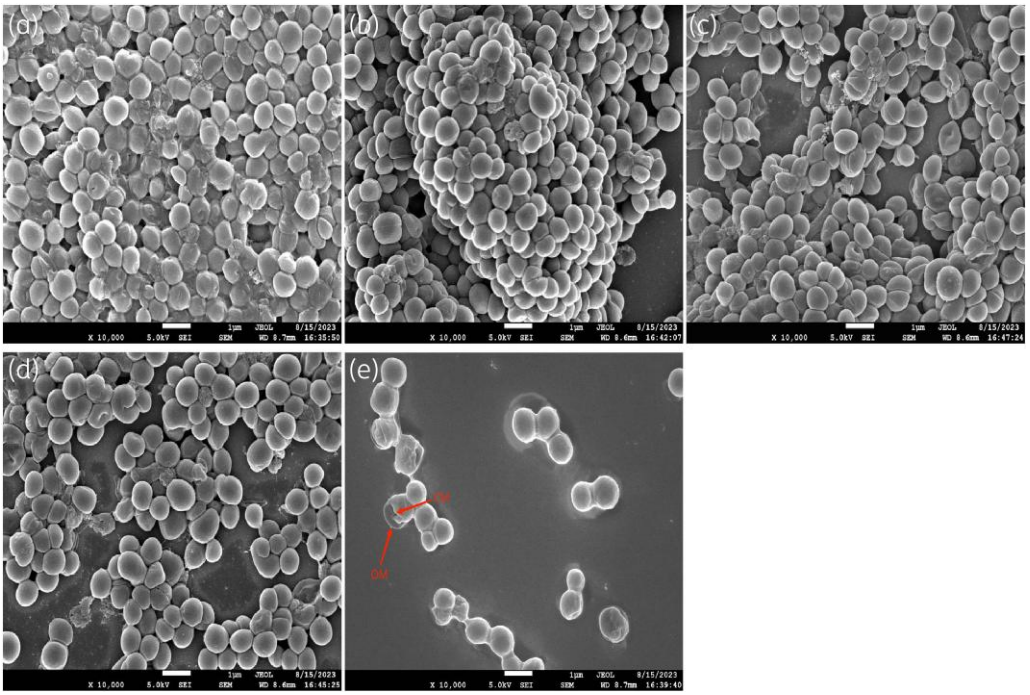

Figure 7. SEM images of MRSA bacterial morphology. (a) Control. (b) Van. (c) Van-MBs. (d) UTMD. (e) Van-MBs + UTMD. The red arrow indicates the morphological changes in the pathogenic microbes. CM, cytoplasmic membrane; OM, outer membrane; the images were further observed at 10 000× magnification.

such as that of K+ channels, alters cytoplasmic osmotic pressure, causing CMs to detach from the OM and leading to cell death. Although it is unclear whether MBs can enter the interior of live MRSA cells and cause changes in bacterial cytoplasmic osmotic pressure, the zeta potentials of MBs and Van-MBs are positively charged on the surface; these MBs can bind to negatively charged bacteria and then combine with ultrasound to exert a cavitation effect, which contributes to the enhancement of bacterial cell membrane permeability. This study suggested that because MBs have a lower positive charge and stick less to the bacterial surface, they have less of an impact on bacteria. Because Van-MBs were more positively charged and more likely to stick to the bacterial surface in large quantities, they had the greatest bactericidal effect when mediated by ultrasonic waves. This more intense cavitation caused plasmic wall separation, which ultimately resulted in bacterial death.

Although the *in vitro* results are promising, they may not fully account for the complex interplay of factors within a living organism. The role of the immune system, the potential development of resistance, and the intricate architecture of biofilms *in vivo* may significantly influence the efficacy of this treatment. Furthermore, the study did not explore the potential systemic effects of high-concentration antibiotic delivery or the long-term implications on bacterial ecology and resistance patterns. Additionally, the impact of different UTMD intervention times on Van release was not investigated, leaving a gap in understanding how timing variations might affect treatment outcomes. Moreover, this study lacks an assessment of the MIC, MBC and MBEC values for the Van-MBs, which are critical for evaluating the effectiveness of this treatment approach.

Conclusion

In summary, Van-MBs have exhibited a superior capacity for penetrating the deeper layer of biofilms. This strategy effectively disrupts biofilm structures by downregulating the icaA gene, which plays a pivotal role in biofilm matrix formation. Additionally, it promotes bactericidal activity through the induction of plasma wall separation, thereby impairing bacterial survival. The innovative application of Van-MBs in conjunction with UTMD has shown considerable promise in addressing the challenges posed by biofilm-associated infections.

Acknowledgements

We thank all authors contributed to the study conception and design. W. B. M. and L. Q. Y. contributed equally to the work described in the article and share first co-author status. All authors read and approved the final manuscript.

Funding

This work was supported by the National Natural Science Foundation of China (no. 82260435), Second Batch of the Tianshan Talent Cultivation Program for Young Promising Talents (2023TSYCQNTJ0003), Key Laboratory of High Incidence Disease Research in Xinjiang (Xinjiang Medical University), Ministry of Education-Key project (2023A01), and State Key Laboratory of Pathogenesis, Prevention and Treatment of High Incidence Diseases in Central Asia (no. SKL-HIDCA-2021-9).

Transparency declarations

The authors have no conflicts of interest to declare.

Author contributions

W. B. M.: Writing—review & editing, Supervision, Funding acquisition. L. Q. Y.: Writing—original draft, Methodology, Data curation. Z. Y. G.: Investigation, Methodology. Y. C. M.: Investigation, Methodology. F. W.: Data analysis. J. H. Y.: Supervision, Funding acquisition.

References

1 Subhadra B, Kim DH, Woo K *et al*. Control of biofilm formation in healthcare: recent advances exploiting quorum-sensing interference strategies and multidrug efflux pump inhibitors. *Materials (Basel)* 2018; **11**: 1676. https://doi.org/10.3390/ma11091676

2 Li Y, Zhang X, Ji B *et al*. One-stage revision using intra-articular carbapenem infusion effectively treats chronic periprosthetic joint infection caused by Gram-negative organisms. *Bone Joint J* 2023; **105-B**: 284–93. https://doi.org/10.1302/0301-620X.105B3.BJJ-2022-0926.R1

3 Karimi A, Karig D, Kumar A *et al*. Interplay of physical mechanisms and biofilm processes: review of microfluidic methods. *Lab Chip* 2015; **15**: 23–42. https://doi.org/10.1039/C4LC01095G

4 Shaw BE, Hahn T, Martin PJ *et al*. National institutes of health hematopoietic cell transplantation late effects initiative: the research methodology and study design working group report. *Biol Blood Marrow Transplant* 2017; **23**: 10–23. https://doi.org/10.1016/j.bbmt.2016.08.018

5 Suran M. Highlights from infectious disease week 2022-COVID-19, HIV, monkeypox, and polio. *JAMA* 2022; **328**: 2089–91. https://doi.org/10.1001/jama.2022.17754

6 Ito A, Taniuchi A, May T *et al*. Increased antibiotic resistance of *Escherichia coli* in mature biofilms. *Appl Environ Microbiol* 2009; **75**: 4093–100. https://doi.org/10.1128/AEM.02949-08

7 Lebeaux D, Ghigo JM, Beloin C. Biofilm-related infections: bridging the gap between clinical management and fundamental aspects of recalcitrance toward antibiotics. *Microbiol Mol Biol Rev* 2014; **78**: 510–43. https://doi.org/10.1128/MMBR.00013-14

8 Mohammadi Mollaahmadi C, Anzabi Y, Shayegh J. Comparison of the frequency of biofilm-forming genes (icaABCD) in methicillin-resistant *S. aureus* strains isolated from human and livestock. *Arch Razi Inst* 2021; **76**: 1655–63. https://doi.org/10.22092/ari.2020.351381.1522

9 Liu J, Chen Y, Wang G *et al*. Improving acute cardiac transplantation rejection therapy using ultrasound-targeted FK506-loaded microbubbles in rats. *Biomater Sci* 2019; **7**: 3729–40. https://doi.org/10.1039/C9BM00301K

10 Kouijzer JJP, Lattwein KR, Beekers I *et al*. Vancomycin-decorated microbubbles as a theranostic agent for *Staphylococcus aureus* biofilms. *Int J Pharm* 2021; **609**: 121154. https://doi.org/10.1016/j.ijpharm.2021.121154

11 Guan L, Wei Y, Du J *et al*. Optimizing the efficacy of targeted gene-loaded ultrasound nanobubbles: an experimental study. *China Med Imaging Technol* 2022; **38**: 1281–5. https://doi.org/10.13929/j.issn.1003-3289.2022.09.001

12 Kot B, Sytykiewicz H, Sprawka I *et al*. Effect of trans-cinnamaldehyde on methicillin-resistant *Staphylococcus aureus* biofilm formation: metabolic activity assessment and analysis of the biofilm-associated genes expression. *Int J Mol Sci* 2019; **21**: 102. https://doi.org/10.3390/ijms21010102

13 Yao L, Mu W, Yuan C *et al*. Effects of vancomycin-loaded microbubbles combined with ultrasound-targeted microbubble disruption on methicillin-resistant *Staphylococcus aureus* biofilms. *Chin J Trauma* 2022; **38**: 923–30. https://doi.org/10.3760/cma.j.cn501098-20220630-00461

14 Welling MM, Warbroek K, Khurshid C *et al*. A radio- and fluorescently labelled tracer for imaging and quantification of bacterial infection on orthopaedic prostheses: a proof of principle study. *Bone Joint Res* 2023; **12**: 72–9. https://doi.org/10.1302/2046-3758.121.BJR-2022-0216.R1

15 Shi K, Zhang H, Gu Y *et al*. Electric spark deposition of antibacterial silver coating on microstructured titanium surfaces with a novel flexible brush electrode. *ACS Omega* 2022; **7**: 47108–19. https://doi.org/10.1021/acsomega.2c06253

16 Bai X, Shen Y, Zhang T *et al*. Anti-biofilm activity of biochanin A against *Staphylococcus aureus*. *Appl Microbiol Biotechnol* 2023; **107**: 867–79. https://doi.org/10.1007/s00253-022-12350-x

17 Chen X, Thomsen TR, Winkler H *et al*. Influence of biofilm growth age, media, antibiotic concentration and exposure time on *Staphylococcus aureus* and *Pseudomonas aeruginosa* biofilm removal in vitro. *BMC Microbiol* 2020; **20**: 264. https://doi.org/10.1186/s12866-020-01947-9

18 Meije Y, Almirante B, Del Pozo JL *et al*. Daptomycin is effective as antibiotic-lock therapy in a model of *Staphylococcus aureus* catheter-related infection. *J Infect* 2014; **68**: 548–52. https://doi.org/10.1016/j.jinf.2014.01.001

19 Kostenko V, Ceri H, Martinuzzi RJ. Increased tolerance of *Staphylococcus aureus* to vancomycin in viscous media. *FEMS Immunol Med Microbiol* 2007; **51**: 277–88. https://doi.org/10.1111/j.1574-695X.2007.00300.x

20 Teirlinck E, Xiong R, Brans T *et al*. Laser-induced vapour nanobubbles improve drug diffusion and efficiency in bacterial biofilms. *Nat Commun* 2018; **9**: 4518. https://doi.org/10.1038/s41467-018-06884-w

21 Kooiman K, Roovers S, Langeveld SAG *et al*. Ultrasound-responsive cavitation nuclei for therapy and drug delivery. *Ultrasound Med Biol* 2020; **46**: 1296–325. https://doi.org/10.1016/j.ultrasmedbio.2020.01.002

22 Walsh TJ, Goodman JL, Pappas P *et al*. Safety, tolerance, and pharmacokinetics of high-dose liposomal amphotericin B (AmBisome) in patients infected with *Aspergillus* species and other filamentous fungi: maximum tolerated dose study. *Antimicrob Agents Chemother* 2001; **45**: 3487–96. https://doi.org/10.1128/AAC.45.12.3487-3496.2001

23 Jefferson KK, Goldmann DA, Pier GB. Use of confocal microscopy to analyze the rate of vancomycin penetration through *Staphylococcus aureus* biofilms. *Antimicrob Agents Chemother* 2005; **49**: 2467–73. https://doi.org/10.1128/AAC.49.6.2467-2473.2005

24 Dong Y, Xu Y, Li P *et al*. Antibiofilm effect of ultrasound combined with microbubbles against *Staphylococcus* epidermidis biofilm. *Int J Med Microbiol* 2017; **307**: 321–8. https://doi.org/10.1016/j.ijmm.2017.06.001

25 Slater RT, Frost LR, Jossi SE *et al*. Clostridioides difficile LuxS mediates inter-bacterial interactions within biofilms. *Sci Rep* 2019; **9**: 9903. https://doi.org/10.1038/s41598-019-46143-6

26 Yang Y, Li H, Sun H *et al*. A novel nitro-dexamethasone inhibits agr system activity and improves therapeutic effects in MRSA sepsis models without antibiotics. *Sci Rep* 2016; **6**: 20307. https://doi.org/10.1038/srep20307

27 Moormeier DE, Bayles KW. *Staphylococcus aureus* biofilm: a complex developmental organism. *Mol Microbiol* 2017; **104**: 365–76. https://doi.org/10.1111/mmi.13634

28 Saadati F, Shahryari S, Sani NM *et al*. Effect of MA01 rhamnolipid on cell viability and expression of quorum-sensing (QS) genes involved in biofilm formation by methicillin-resistant *Staphylococcus aureus*. *Sci Rep* 2022; **12**: 14833. https://doi.org/10.1038/s41598-022-19103-w

29 Arciola CR, Baldassarri L, Montanaro L. Presence of *icaA* and *icaD* genes and slime production in a collection of staphylococcal strains from catheter-associated infections. *J Clin Microbiol* 2001; **39**: 2151–6. https://doi.org/10.1128/JCM.39.6.2151-2156.2001

30 Pokharel K, Dawadi BR, Shrestha LB. Role of biofilm in bacterial infection and antimicrobial resistance. *JNMA J Nepal Med Assoc* 2022; **60**: 836–40. https://doi.org/10.31729/jnma.7580

31 Kang W, Liang J, Liu T *et al*. Preparation of silane-dispersed graphene crosslinked vinyl carboxymethyl chitosan temperature-responsive hydrogel with antibacterial properties. *Int J Biol Macromol* 2022; **200**: 99–109. https://doi.org/10.1016/j.ijbiomac.2021.12.050

32 Luo J, Yang P, Cheng J *et al*. Photosensitizers with aggregation-induced far-red/near-infrared emission for versatile visualization and broad-spectrum photodynamic killing of pathogenic microbes. *J Colloid Interface Sci* 2023; **634**: 664–74. https://doi.org/10.1016/j.jcis.2022.12.062